Electron mobility in Ge and strained- Si channel ultrathin-body metal-oxide semi conductor field-effect transistors

Tony Low, M. F. Li, Chen Shen, Yee-Chia Yeo, Y. T. Hou, Chunxiang Zhu, Albert Chin, and D. L. Kwong

---

Articles you may be interested in

Improvement of subthreshold swing of n -channel transistor by uniaxial tensile stress due to a quantum mechanical mechanism instead of physical thinning
Appl. Phys. Lett. **94**, 173503 (2009); 10.1063/1.3125248

Drive current enhancement in p -type metal–oxide–semiconductor field-effect transistors under shear uniaxial stress
Appl. Phys. Lett. **85**, 6188 (2004); 10.1063/1.1841452
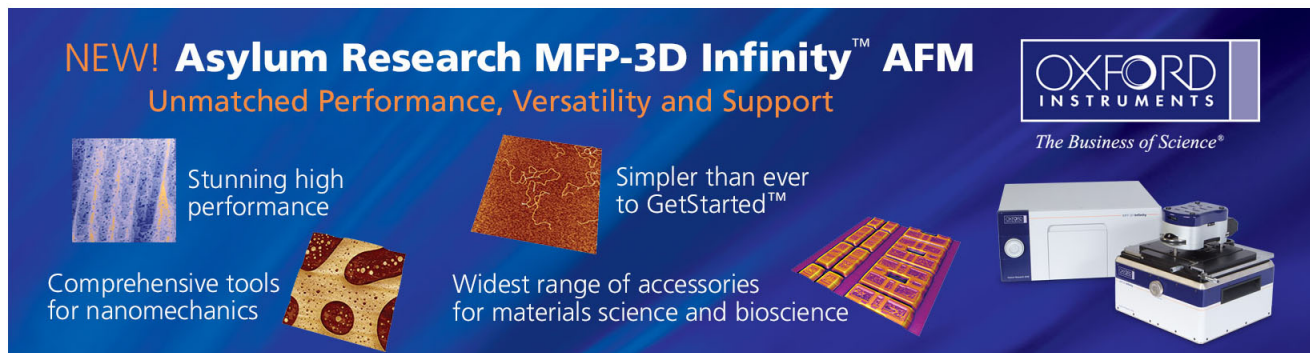
Evidence of Si SiGe heterojunction roughness scattering
Appl. Phys. Lett. **85**, 4947 (2004); 10.1063/1.1828224

Monte Carlo based analysis of intermodulation distortion behavior in GaN–Al x Ga 1x N high electron mobility transistors for microwave applications
J. Appl. Phys. **90**, 3030 (2001); 10.1063/1.1390495

Surface roughness at the Si–SiO 2 interfaces in fully depleted silicon-on-insulator inversion layers
J. Appl. Phys. **86**, 6854 (1999); 10.1063/1.371763

Electron mobility in Ge and strained-Si channel ultrathin-body metal-oxide semi conductor field-effect transistors

Tony Low, M. F. Li,[a)] Chen Shen, Yee-Chia Yeo, Y. T. Hou, and Chunxiang Zhu
Silicon Nano Device Laboratory, Department of Electrical and Computer Engineering National University of Singapore and Institute of Microelectronics, Singapore 119260, Singapore

Albert Chin
Department of Electronics Engineering, National Chiao Tung University, Taiwan

D. L. Kwong
Department of Electrical and Computer Engineering, University of Texas, Austin, Texas 78752

Electron mobility in strained silicon and various surface oriented germanium ultrathin-body (UTB) metal-oxide semiconductor field-effect transistors (MOSFETs) with sub-10-nm-body thickness are systematically studied. For biaxial tensile strained-Si UTB MOSFETs, strain effects offer mobility enhancement down to a body thickness of 3 nm, below which strong quantum confinement effect renders further valley splitting via application of strain redundant. For Ge channel UTB MOSFETs, electron mobility is found to be highly dependent on surface orientation. Ge$\langle 100 \rangle$ and Ge$\langle 110 \rangle$ surfaces have low quantization mass that leads to a lower mobility than that of Si in aggressively scaled UTB MOSFETs. © *2004 American Institute of Physics.* [DOI: 10.1063/1.1788888]

Ultrathin-body (UTB) transistors with sub-10-nm-body thickness T_{body} is a promising candidate for device scaling into the sub-30-nm gate length L_G regime. However, degradation of electron mobility in UTB devices with sub-10-nm T_{body} was found experimentally.[1,2] Degration of mobility also leads to reduce current drivability in the linear regime[3] despite the improved gate inversion layer capacitive coupling with reduced body scaling.[3] Of particular concern is current drivability under high drain biases for decananometer channel length devices. With regard to this, Lundstrom[4] has pointed out, via a phenomenological approach, that the transport in decananometer metal-oxide semiconductor field-effect transistor (MOSFETs) is essentially source limited; hence the mobility at high vertical surface field, which embodies the effective scattering rate in the vicinity of the source, remains relevant. In addition, recent reports on aggressively scaled UTB devices have highlighted the importance of the interfacial perturbation attributed to the roughness of the Si/SiO_2 surface,[2,5] which is found to strongly limit the carrier mobility. For enhanced device performance, channel materials such as Ge and strained-Si (formed directly on insulator without a relaxed SiGe buffer layer) may be employed in UTB transistor.[6,7] Nevertheless, there is little work on their potential advantages. Little is also known about the carrier mobility in these UTB devices with advanced channel materials. In this letter, we perform a modeling study of the electron mobility in UTB transistor with sub-10-nm-body thicknesses employing strained-Si and various surface orientations of Ge as the channel material. A calibrated physical model that takes the effect of scattering due to optical phonons, acoustic phonons, surface roughness, and interface states into account is used.

Electronic structures for the two-dimensional electron gas are obtained by solving the coupled Schrödinger–Poisson equation self-consitently within the envelope function based effective mass framework according to Stern *et al.*[8] Important bandstructure parameters such as the conduction valleys energy minima and their longitudinal and transverse masses used are obtained from Fischetti *et al.*[9] A unitary transformation is employed[8,10] to obtain the transport masses along the device coordinates for devices with various crystal orientations. The 2D density-of-states mass is preserved after the transformation in our context of low longitudinal field. The scattering matrix elements due to acoustic phonons (AP), optical phonons (OP), surface roughness (SR), and interface states (DIT) related scattering are then systematically formulated. The model for phonon spectrum in the bulk semiconductors are adapted from Jacoboni *et al.*[11,12] where the matrix elements of the electron-phonon interaction are considered in accordance with Price[11,13,14] Intravalley acoustic phonon (AP) with an effective isotropic deformation potential[11,15,16] intravalley optical phonon (OP) for L valleys[11,12] and intervalley phonons constraint within the selection rules for f and g type processes[11] are accounted for. Dynamic screening of phonons is disregarded.[17] Surface roughness (SR) scattering was conventionally treated by accounting for the localized perturbation potential due to variations of interface positions according to Ando's.[18–20] The perturbation Hamiltonian induced by energy level fluctuations has been obtained[21,22] for a rectangular quantum well potential, but this approach may not be accurate for the treatment of surface roughness in UTB devices. Issues also remain about the accurate treatment of perturbation potential due to change in charge density induced by SR. Consequently, we employed a phenomenological treatment as outlined by Gamiz.[23] The autocorrelation function of the asperities is assumed to be Gaussian. Intersubband transitions are left unscreened and the dielectric matrix is expressed according to Ref. 14 and in the quantum size limit when applicable, else it is left unscreened. Interface state (DIT) induced scattering potential according to Stern *et al.*[8] based on a perturbative approach is employed. By imposing appropriate boundary conditions, the scattering potential in all regions of interest can be obtained

---
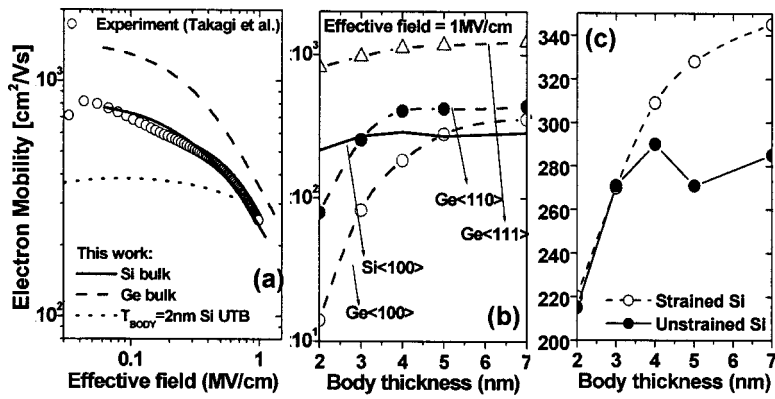a)Electronic mail: elelimf@nus.edu.sg

FIG. 1. (a) Calibration of our theoretical low-field mobility model with experimental results for Si (Ref. 24). Theoretical calculated mobility for a 2 nm T_{body} Si UTB MOSFET is also shown. Screening for SR scattering is accounted. (b) Electron mobility for various advanced channel UTB transistors as function of body thickness. Si channel is oriented in [010] direction. Ge$\langle 100 \rangle$ is oriented along [010] channel direction, Ge$\langle 110 \rangle$ at [$1\bar{1}0$] and Ge$\langle 111 \rangle$ is isotropic. We ignored the neighboring Δ valley in this work. (c) replots the mobility curve in linear scale for the Si$\langle 100 \rangle$ curve in the main figure. A peak is clearly shown, in good agreement with the experiment (See Refs. 1 and 2). A mobility curve for strained Si$\langle 100 \rangle$ is also plotted for comparison.

using the Nystrom method.[15] The scattering rate can be obtained by the Fermi Golden Rule. We then obtained the numerical solutions of the scattering time to the Boltzmann equation in the Ohmic regime by embracing the relaxation time approximation and imposing the appropriate scattering condition under detailed balance condition at equilibriums.[15,16]

Our physical model is calibrated using experimental Si mobility data,[24] showing good agreement [Fig. 1(a)]. An effective acoustic deformation potential of 15 eV[14,15] was used. As current processing technology is still unable to yield a reliable set of mobility data for Ge MOSFETs, a deformation potential of 15 eV for acoustic phonon intravalley process within valleys is assumed, yielding a reasonable two times mobility compared to Si counterpart[25,26] as shown in Fig. 1(a). A SR autocorrelation function with root mean square $\Delta = 4$ Å and correlation length $l = 10$ Å is assumed for Si and Ge[7] surfaces. These technologically dependent parameters are assumed to apply to UTB transistor technology. A conservative interface states density of 1×10^{11} cm^{-2} for each of the front and back interfaces is assumed. Our UTB device has a gate dielectric with an EOT of 1 nm, a metal gate electrode (which provides efficient charge screening), and back oxide thickness of 50 nm. The mobility for a 2 nm T_{body} Si UTB MOSFET is calculated as shown in Fig. 1(a). It is observed that its electron mobility at high surface field does not exhibit the same dependency on effective field as the bulk universal mobility. Perturbation Hamiltonian due to SR H_{SR} as obtained to first order approximation is:

$$H_{SR}(z,\mathbf{r}) \cong \frac{q_0[V(z,\Delta_m) - V(z,0)]\Delta(\mathbf{r})}{\Delta_m}, \tag{1}$$

where the coordinates z (perpendicular to Si/SiO$_2$ interface, measured from back oxide interface) and $\mathbf{r}$ (vector in the plane of the Si/SiO$_2$ interface) are employed. $\Delta(\mathbf{r})$ is a function which effectively describes the sum of SR at the two interfaces and Δ_m is the statistical mean of the SR. $V(z,\Delta_m)$ is the electrostatic potential with a surface perturbation of Δ_m, which is also solved self-consistently accounting for the finite body thickness fluctuation Δ_m. However, at large body thickness, one obtains

$$T_{body \to \infty}^{lim} H_{SR} \cong q_0 \frac{V(z+\Delta_m, 0) - V(z,0)}{\Delta_m} \Delta(\mathbf{r}) \cong q_0 \frac{\partial V}{\partial z}\Delta(\mathbf{r}), \tag{2}$$

where H_{SR} is now proportional to the surface field $\partial V/\partial z$, accounting for the usual dependence of surface roughness limited mobility on effective field $\sim F_{eff}^2$ in the bulk

Si MOSFET. When T_{body} in the order of SR, deviation from usual electric field dependency is captured by H_{SR} in Eq. (1).

The electron mobility as a function of T_{body} is calculated for strained Si (with biaxial tensile strain of 2%, considerably larger based on current technology) and Ge with different surface orientations, as shown in Fig. 1(b). At high effective field of 1 MV/cm, SR induced scattering dominates the effective mobility. The limited mobilities due to AP, OP, SR, and DIT are also calculated as a function of T_{body} (Fig. 2), clearly indicating the dominance of SR limited mobility at an effective field of 1 MV/cm. The application of strain is found to lose its effectiveness at ~3 nm of T_{body} as shown in the inset of Fig. 1(c). This is because, at small T_{body}, strong quantum confinement lifts the Δ_4 valleys much beyond that of the high mobility Δ_2 valleys, rendering further valley splitting via application of strain redundant. It has been assumed that the SR spectrum function in strained or un-
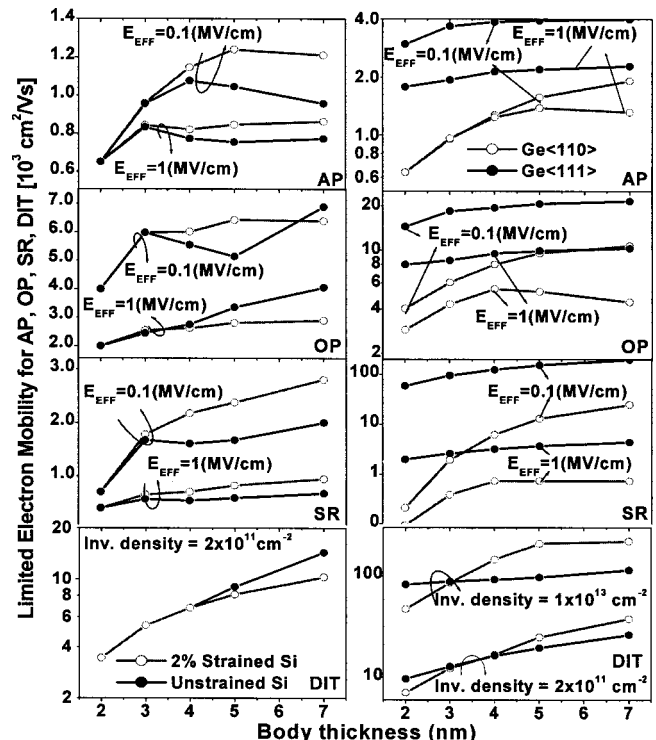

FIG. 2. Limited low field mobilities for strained Si and Ge UTB transistor, respectively. Acoustic phonons, optical phonons, SR, and interface charge limited mobilities are all systematically explored. All limited mobilities are plotted at constant effective field of 0.1 MV/cm (threshold condition) and 1 MV/cm (high inversion condition) except for interface charge limited mobility plotted at a constant electron density criterion.
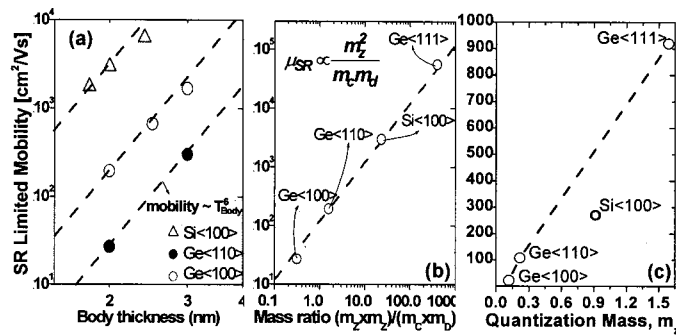
FIG. 3. (a) SR limited mobility plotted at effective surface field of 0.1 MV/cm, exhibiting approximately the T_{body}^6 dependency, (b) surface roughness limited mobility at effective surface field of 0.1 MV/cm as function of mass ratio as expressed in inset, with T_{body} =2 nm under same SR condition. (c) Electron mobility as function of quantization mass m_z. Simulated at T_{body}=2 nm and E_{eff} =1 MV/cm. High quantization mass m_z, is beneficial for aggressively scaled UTB device.

strained Si devices are the same. Of particular interest is the choice of channel surface orientations for optimum device performance. Figure 1(b) compares the total effective mobility of Ge and Si channel UTB devices with T_{body} of sub-10-nm. Interestingly, while the electron mobility in bulks Ge is higher than that in bulk Si, Ge⟨110⟩ and Ge⟨100⟩ UTB devices have lower mobility than Si⟨100⟩ at T_{body} below 3 nm. Ge⟨111⟩ shows better mobility than Si⟨100⟩ at all body thicknesses. Generally, it is observed that at sufficiently thin T_{body}, the electron mobility begins to degrade. The onset and amount of this degradation differs for the various orientations.

Sakaki *et al.*[22] has established the SR limited mobility with a T_{body} to a power of 6 dependency for the of quantum well.[22] Uchida *et al.* have also experimentally verified this dependency for Si UTB with small T_{body} at low inversion charge condition.[2] Our model predicts a similar dependency on T_{body} for the SR mobility at a low constant surface field of 0.1 MV/cm, as shown in Fig. 3(a). In addition, the SR limited mobility for UTB with small T_{body} at low constant surface field approximately follows a mass ratio relationship as elucidated in Fig. 3(b). However, since SR scattering dominates in the high effective surface field regime, it is of paramount importance to examine their mobility in this regime, where SR induced charge perturbation will contribute additional SR perturbation potential. Figure 3(c) plots the electron mobility at high effective surface field as a function of quantization mass for the various channel materials. A general trend of decreasing electron mobility with reduced quantization mass can be observed. This can be phenomenologically explained by the effect of quantization mass on the screening of potential. A larger quantization mass causes the carriers to be nearer to the interface resulting in more efficient potential screening. This reduces the overall SR perturbation potential. Conversely, a small quantization mass will render very sensitive to the SR condition.

In summary, the electron mobility of UTB MOSFETs with sub-10-nm T_{body} and advanced channel materials are systematically studied. At small T_{body}, Ge⟨100⟩ and Ge⟨110⟩ suffer large mobility degradation due to their very low quantization masses, resulting in high susceptibility to SR scattering. Ge⟨111⟩ with its large quantization mass and low density of state mass is highly desirable for high mobility in the ultrathin-body regime.

[1] K. Uchida, J. Koga, R. Ohba, T. Numata, and S. Takagi, Tech. Dig. - Int. Electron Devices Meet. **2001**, 633 (2001).

[2] K. Uchida, H. Watanabe, A. Kinoshita, J. Koga, T. Numata, and S. Takagi, Tech. Dig. - Int. Electron Devices Meet. **2002**, 47 (2002).

[3] See Ref. 1. Figure 10 shows the enhanced inversion layer capacitances with body scaling from 25 to 7 nm. Figure 13 shows the degradation of current drivability in linear regime, attributing mainly to degradation of low-field mobility.

[4] M. S. Lundstrom, IEEE Electron Device Lett. **22**, 293 (2001).

[5] Z. Ren, P. M. Solomon, T. Kanarsky, B. Doris, O. Dokumaci, P. Pldigies, R. A. Roy, E. C. Jones, M. Leong, R. J. Miller, W. Haensch, and H. S. Wong, Tech. Dig. - Int. Electron Devices Meet. **2002**, 51 (2002).

[6] K. Rim, K. Chan, L. Shi, D. Boyd, J. Ott, N. Klymko, F. Cardone, L. Tai, S. Koester, M. Cobb, D. Canaperi, B. To, E. Duch, I. Babich, R. Carruthers, P. Saunders, G. Walker, Y. Zhang, M. Steen, and M. Leong, Tech. Dig. - Int. Electron Devices Meet. **2003**, 49 (2003).

[7] S. Nakaharai, T. Tezuka, N. Sugiyama, Y. Moriyama, and S. Takagi, Appl. Phys. Lett. **83**, 3516 (2003).

[8] F. Stem and W. E. Howard, Phys. Rev. **163**, 816 (1967).

[9] M. V. Fischetti and S. E. Laux, J. Appl. Phys. **80**, 2234 (1996), see Figs. 1 and 4.

[10] A. Rahman, A. Ghosh, and M. Lundstrom, Tech. Dig. - Int. Electron Devices Meet. **2003**, 471 (2003).

[11] C. Jacoboni and L. Reggiani, Rev. Mod. Phys. **55**, 645 (1983).

[12] C. Jacoboni, F. Nava, C. Canali, and G. Ottaviani, Phys. Rev. B **24**, 1014 (1981).

[13] P. J. Price, Ann. Phys. (San Diego) **133**, 217 (1981).

[14] C. Jungemann, A. Emunds, and W. L. Engl, Solid-State Electron. **36**, 1529 (1993).

[15] D. Esseni and A. Abramo, IEEE Trans. Electron Devices **50**, 1665 (2003).

[16] D. Esseni, A. Abramo, L. Selmi and E. Sangiorgi, Tech. Dig. - Int. Electron Devices Meet. **2002**, p 719 (2002).

[17] M. V. Fischetti, and S. E. Laux, Phys. Rev. B **48**, 2244 (1993).

[18] T. Ando, J. Phys. Soc. Jpn. **43**, 1616 (1977).

[19] T. Ando, A. B. Fowler, and F. Stern, Rev. Mod. Phys. **54**, 437 (1982).

[20] D. Esseni, IEEE Trans. Electron Devices **51**, 394 (2004).

[21] C. Y. Mou and T. M. Hong, Phys. Rev. B **61**, 12612 (2000).

[22] H. Sakaki, T. Noda, K. Hirakawa, M. Tanaka, and T. Matsusue, Appl. Phys. Lett. **51**, 1934 (1987).

[23] F. Gamiz, J. B. Roldan, J. A. Lopez-Villanueva, P. Cartujo-Cassinello, and J. E. Carceller, J. Appl. Phys. **86**, 6854 (1999).

[24] S. Takagi, A. Toriumi, M. Iwase, and H. Tango, IEEE Trans. Electron Devices **41**, 2357 (1994).

[25] C. M. Ransom, T. N. Jackson, and J. F. DeGelormo, IEEE Trans. Electron Devices **38**, 2695 (1991).

[26] C. H. Huang, D. S. Yu, A. Chin, C. H. Wu, W. J. Chen, C. Zhu, M. F. Li, B. J. Cho, and D. L. Kwong, Tech. Dig. - Int. Electron Devices Meet. **2003**, 319 (2003).